Scientific Research Publishing

Open Journal of Biophysics, 2024, 14, 99-120
https://www.scirp.org/journal/ojbiphy
ISSN Online: 2164-5396
ISSN Print: 2164-5388

Phytochemicals of *Aloe barbadensis miller* as Potential Inhibitors of Uropathogenic *Escherichia coli* for Urinary Tract Infection Therapy: An *in Silico* Approach

Mikidadi Salehe Gurisha, Pulapa Venkata Kanaka Rao, Laxmikanth Cherupally

Department of Physics, College of Natural and Mathematical Sciences, University of Dodoma, Dodoma, Tanzania
Email: *salehegs@gmail.com

How to cite this paper: Gurisha, M.S., Rao, P.V.K. and Cherupally, L. (2024) Phytochemicals of *Aloe barbadensis miller* as Potential Inhibitors of Uropathogenic *Escherichia coli* for Urinary Tract Infection Therapy: An *in Silico* Approach. *Open Journal of Biophysics*, **14**, 99-120.
https://doi.org/10.4236/ojbiphy.2024.142006

Received: December 27, 2023
Accepted: February 4, 2024
Published: February 7, 2024

Abstract

Urinary tract infections (UTIs) are common infections caused by normal skin or rectum bacteria that get into the urethra and infect the urinary tract. Although the infection can affect various parts of the tract, bladder infections are the most prevalent kind. Uropathogenic *Escherichia Coli* (UPEC) is the most common pathogen associated with UTI development. Therefore, inhibiting the UPEC protein target (PDB ID: 8BVD) appears to be a promising therapeutic strategy. Therefore, in this study, molecular docking and dynamics were conducted to examine the antibacterial activity of *Aloe barbadensis miller* against UPEC bacteria. The *Aloe barbadensis miller* natural compounds licochalcone A, palmidin B and palmidin C were downloaded from PubChem with amoxicillin, which was used as a control drug and studied against the target molecule. The potential parameters examined were the docking scores, absorption, distribution, metabolism, excretion, toxicity (ADMET), bioavailability, root mean square deviation (RMSD), root mean square fluctuation (RMSF), hydrogen bonding, radius of gyration, and potential energy of the system. Docking scores showed that all ligands demonstrated an admirable candidature as an inhibitor to 8BVD molecule, and the score hierarchy is licochalcone A (−6.4 kcal/mol), palmidin C (−6.1 kcal/mol), palmidin B (−6.0 kcal/mol), and amoxicillin (−5.9 kcal/mol). All ligands appeared to have good drug-like properties and oral bioavailability. Molecular dynamic studies showed that all ligands exhibited an excellent nominee as inhibitors in their vicinity at 20 ns. However, there is a relatively high fluctuation of palmidin B compared with other compounds, which seems to be more stable. This work suggests that the selected phytoconstituents could be used as inhibitors of the 8BVD protein in the fight against UTIs. However, further

investigation on the clinical and experimental validation of UTI treatment's specific mechanisms and effects is still welcomed.

Keywords

Uropathogenic *Escherichia Coli*, Phytochemicals, Molecular Docking, Ligand, Hydrogen Bond

1. Introduction

Urinary tract Infections (UTIs) are usually recognized as one of the most prevalent bacterial infections among various patient populations, especially in females, where more than 80% develop one in their lifetime and more than 20% - 50% experience recurrence episodes [1] [2]. It has been recognized as the second most frequently misdiagnosed illness and the second most prevalent contagious condition after pneumonia. More lately, it has developed into a severe health issue affecting people, with almost 150 million cases worldwide per annum and a disproportionate financial burden on the world economy [3] [4]. UTIs are classified into two clinical categories: complicated and non-complicated type. Non-complicated UTIs are associated with the health of patients showing the absence of structural or neurological urinary tract abnormalities while complicated UTIs are linked to factors that compromise the urinary tract or host defense, including immunosuppression, renal failure, pregnancy, urinary blockage, urine retention, and indwelling catheters or other drainage [5] [6]. Several factors contribute to UTIs development, especially for premenopausal women which include blood group, history of childhood UTIs family history, changes in bacterial flora, and sexual intercourse [7].

Uropathogenic *Escherichia coli* (UPEC) is the culprit behind urinary tract infections [8]. A specialized virulence factor in UPEC stains allows bacteria to thrive and spread in urine and other extra-intestinal settings as well as infiltrate host tissues [9]. The primary virulence-causing substances that depend on the UPEC are adhesions (type 1 fimbriae, curli fimbriae, flagellum, afimbrial adhesion, and p fimbriae), aerobactins, hemolysins, and cytotoxic necrotizing factor [10]. The bacteria possess stains that transform from their commensal condition when intestinal flora develops and persist in the urine tract. They also display a wide range of virulence factors and techniques, allowing them to infect and cause infections in the urinary tract [11].

Antibiotic medications such as trimethoprim, lactams, fluoroquinolones, nitrofurantoin, and amoxicillin are most frequently used for the treatment of uncomplicated UTIs in many developing countries [12]. However, the effectiveness of some of these drugs is currently being eroded by antibiotic resistance, which leads to treatment failure, prolonged sickness, and an increased risk of mortality when treating illnesses brought on by resistant microorganisms [13]. A drug like amoxicillin has been used as the second-line empirical treatment in many Afri-

can health centers and dispensaries for treating UTIs despite the recommendations prescribed by the Infectious Diseases Society of American (IDSA) guidelines 1999 [14].

Phytochemicals originating from natural products have been used by pharmacologists in drug development, the products have been carefully used in the laboratory search for innovative drugs in combination with other techniques such as computer modeling [15]. Molecular docking and molecular dynamics have been identified as effective techniques used in searching for new drugs and are thus widely used in the pharmaceutical industry [16]. The computational approach can be used in direct studies, interpretation and to speed up the development of drugs [17]. The methodology ensures that the best lead molecule may undergo animal studies, which might reduce costs associated with drug discovery and speed up the time it takes for a medicine to reach the consumer market [18] [19].

Many human infectious disorders have recently been treated with medicinal plants with antibacterial and anti-inflammatory properties [19]. Aloe vera (*Aloe barbadensis miller*) is a well-known therapeutic plant used against UPEC [20]. Its Phytochemicals have major pharmacological features and are frequently safer and more chemically diverse than synthetic prescription medications acquired from commercial sources [21]. Because of this, they are becoming more famous among clinical researchers as a way to offer quick and inexpensive therapeutic solutions for treating urinary tract infections [21] [22].

Therefore, this work used computational methods to determine the antibacterial activities of licochalcone A, palmidin B, palmidin C, and amoxicillin as a control drug to assess crucial factors such as docking score, absorption, distribution, metabolism, excretion, toxicity (ADMET), bioavailability, root mean square deviation (RMSD), root mean square fluctuation (RMSF), hydrogen bonding, radius of gyration and potential energy of the system.

2. Materials and Methods

2.1. Target Protein Preparation

The Protein target of Uropathogenic *Escherichia coli* (UPEC) type 1 fimbrial (FimH) lectin domain in complex with mannose C-linked to quinolone was retrieved from the Protein Data Bank (PDB ID 8BVD) (https://www.rcsb.org/) (**Figure 1**) [23]. The targeted macromolecule was obtained using the X-ray diffraction method with a resolution of 3.00 Å, R-value free of 0.303, and R-value work of 0.251, which gives the molecule good quality with high resolution [24]. UPEC type 1 FimH complex molecules are attractive alternatives to antibiotic treatments and preventive measures against acute or recurrent urinary tract infections (UTIs) [25] [26]. Ucsf Chimera software was used to prepare protein receptors by removing the unwanted ligand and solvent molecules from the 8BVD target, eliminating the alternative location of residues, changing selenomethionines to methionines, adding hydrogen atoms, and assigning charges to

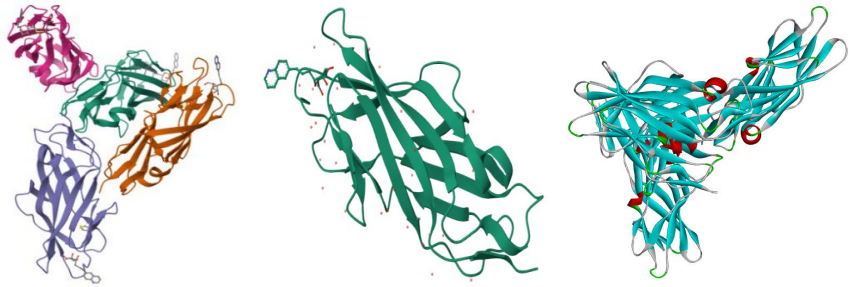

(a) (b) (c)

Figure 1. (a) & (b) are the general structure of FimHlectin domain in 2 and 3 D and (c) is the 8BVD receptor target.

the protein atoms [27]. The ligand coordinates for site-specific docking were assigned, for the center at X: 26, Y: 58, Z: −9, and for a box of dimension X: 13, Y: 7, Z: 10. The prepared protein receptor was saved in a mol 2 file ready for docking.

2.2. Ligand Preparation

The natural compounds of aloe vera (*aloe barbadensis miller*) were retrieved from an accessible commercial PubChem library (https://pubchem.ncbi.nlm.nih.gov/) (**Figure 2**). Ucsf Chimera software was used to prepare the ligands by optimizing it as equal to the protein was optimized and saved as mol 2 in the working directorate [28].

2.3. Molecular Docking

Molecular docking was performed in the Ucsf chimera by selecting the protein receptor, minimizing the ligands saved in the mol2 file, and opening them in the Auto Dock Vina window. The receptor and ligand were selected as outputs, and the coordinates for the center and the size for site-specific docking were generated in the boxes. The executable location path for the vina and vina splits was set and docking was performed.

2.4. Physicochemical, Pharmacokinetics, Drug-Likeness and ADMET Prediction

The physicochemical properties of a drug play a significant role in determining its pharmacokinetic and pharmacodynamic profiles, which are essential for increasing a drug candidate's chances of success during the preclinical development process [29]. Drug candidates fail in clinical trials for a variety of reasons, but the two main reasons are undesirable pharmacokinetic characteristics and unacceptable toxicity [30]. Therefore, it is essential for scholars to select candidates with the correct balance of potency, absorption, distribution, metabolism, excretion, and toxicity (ADMET) [31]. In contrast, pharmacokinetics are undoubtedly caused in part by the inhibition of these isoenzymes (CYP1A2, CYP2C19, CYP2C9, CYP1A2, CYP2D6, and CYP3A4). Because of the decreased

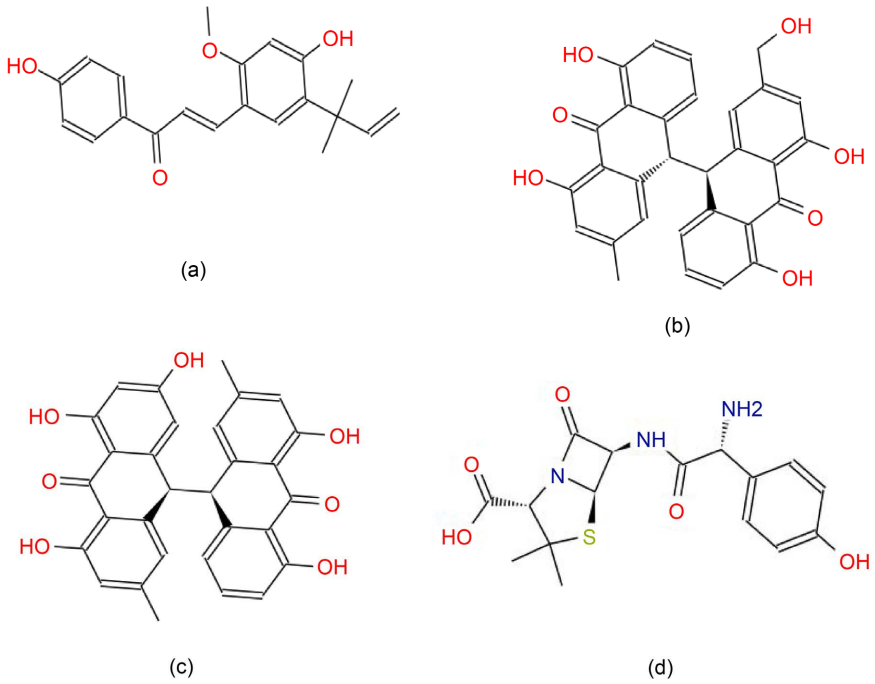

Figure 2. Molecular structures of the compounds (a) licochalconeA, (b) palmidin B, (c) palmidin C and (d) amoxicillin.

clearance and accumulation of the drug or its metabolites, related drug-drug interactions may produce toxic or other negative side effects. The compounds used in this study were assessed: pharmacokinetic (pk), physicochemical, drug-Likeness and ADMET prediction using pkCSM and SwissADME web tools [32] [33].

2.5. Bioavailability Radar

Drug likenesses are quickly assessed by using bioavailability radar, in this case, six physiochemical parameters like lipophilicity, size, polarity, solubility, flexibility, and saturation were considered [34]. Comprehensive and truthful tests were performed using SwissADME software.

2.6. Molecular Dynamics

Molecular dynamics (MD) are frequently used to study large molecules like proteins which can be utilized to ascertain conformational space [35]. In this case, molecular dynamics was performed to examine the actual motion of atoms, which aids in understanding the detailed interaction of 8BVD with potential phytochemicals, especially when it binds to a protein target [36]. Several biological activities and intricate dynamic processes have not been identified by observing the internal dynamics of proteins [37]. The GROMACS (gmx 2023. 1) software was used to perform molecular dynamics simulations on 8BVD-CID5318998, 8BVD-CID 5320385, 8BVD-CID 5320386, and 8BVD-CID 33613 at 300 K with a CHARMM27 force field, and the hybrid ligand structure and force field properties of the chosen ligand were determined using SwissPa-

ram [38].

Free 8BVD, 8BVD-CID5318998, 8BVD-CID5320385, 8BVD-CID5320386, and 8BVD-CID 33613 were solvated with water in a cubic box with a basic diameter of 1 nm with all default settings. The temperature of the entire system was increased from 0 to 300 K during the length of the equilibration time (1000ps) while maintaining a steady volume and periodic boundary conditions, and the system was then reduced using the 1000 sharpest decline steps. The generated trajectories were used to assess the behavior of each complex and stability of the overall system. Calculations of the hydrogen bond, root mean square deviation, root mean square fluctuation, radius of gyration, and potential energy were used to examine the variations in the macromolecule and macromolecule-ligand complex system [39]. The number of particles, system volume and temperature (NVT) ensemble, number of particles, system pressure, and temperature (NPT) ensemble were used to separate the equilibration process into two phases. While all the other atoms were allowed to move freely in both NVT and NPT, the C backbone atoms of the original structures were constrained. Molecular dynamics (MD) was then run at 300 K with a 20 ns time frame. The trajectories obtained were examined using the GROMACS analysis modules. UCF Chimera and Maestro were used to visualize MD movies and interaction diagrams, respectively [40].

3. Results and Discussion

3.1. Docking Scores

Molecular docking scores for licochalcone A, palmidin B, palmidin C and Amoxicillin presented in (**Table 1**), the scores revealed that licochalcone A ligand has the lowermost binding affinity toward the 8BVD target. A lower docking score indicates that ligand and target binding are more stable. The different structures bound to the target caused variations in ligand-target interactions (**Figure 3**), which led to different docking scores [41]. Small molecules of licochalcone A have been reported as potential lead drugs for the treatment of bacterial infections [42].

The poses for each ligand-target interaction were compared to perform visual analysis. The protein-active sites were designed to accommodate ligand interactions. At first, the analysis of the licochalcone-target, in which its 2D projection

Table 1. Docking score for ligand-protein target.

PubChem ID	Molecular Formula	Name	Docking Scores (kcal/mol)
5318998	$C_{21}H_{22}O_4$	Licochalcone A	−6.4
5320385	$C_{30}H_{22}O_7$	Palmidin B	−6.0
5320386	$C_{30}H_{22}O_7$	Palmidin C	−6.1
33613	$C_{16}H_{19}N_3O_5S$	Amoxicillin	−5.9

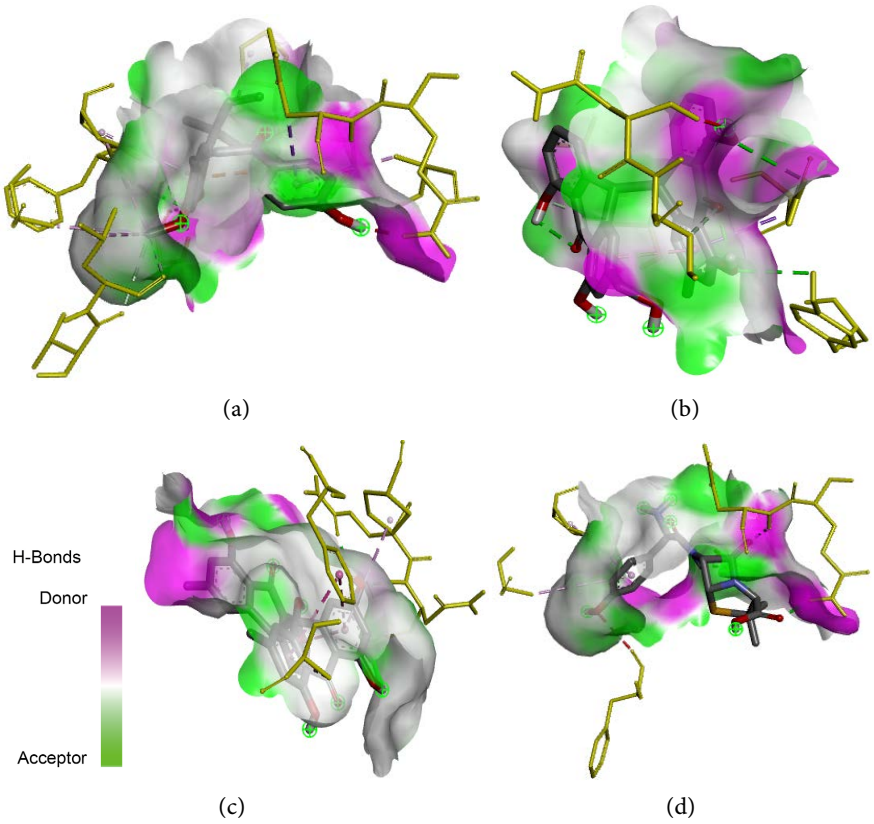

Figure 3. A 3D Hydrogen bond interaction map of the 8BVD-Ligand: (a) Licochalcone A, (b) Palmidin B, (c) Palmidin C, (d) Amoxicillin.

interaction is shown in **Figure 4(a)**, was discussed. One OH group in licochalcone A ligand form hydrogen bonds with protein residues Asp47 and Asp54. In this case licochalcone A acts as a hydrogen donor to the polar residues Asp54 whereas it acts as an acceptor to the amino acid residues Asp47.The bond formed here is somewhat complicated, where licochalcone A acts as a hydrogen donor and acceptor simultaneously. It also form hydrophobic interaction with Tyr49 amino acid residues.

The second pose is the palmidin B-target interaction, as shown in **Figure 4(b)**. The figure displays that Palmidin B forms three OH groups in the form of hydrogen bonds with Asp47, Asp54, Asn46, Phe1, G1n33 and Asp140. In this case, the Asp140 and Asn54 polar residues acts as a hydrogen acceptor, while the amino acid residues Asp47, Asn46, Gln33 and Phe1 act as donors to palmidin B oxygen atoms. It is estimated that the docking score of palmidin B is more positive than that of licochalcone A owing to the interaction of two hydrogen bonds with the Asp140 polar residue. On the other hand, palmidin B form hydrophobic interaction with Tyr137polar residue.

The third pose is palmidin C-target interaction, as shown in **Figure 4(c)**. The figure clarifies that palmidin C forms one OH group in the form of a hydrogen bond with Asp140, Asn135 and Gln133. In this case, the Asp140 polar residue acts as a hydrogen bond acceptor, whereas Asn135 and Gln133 acts as a donor to

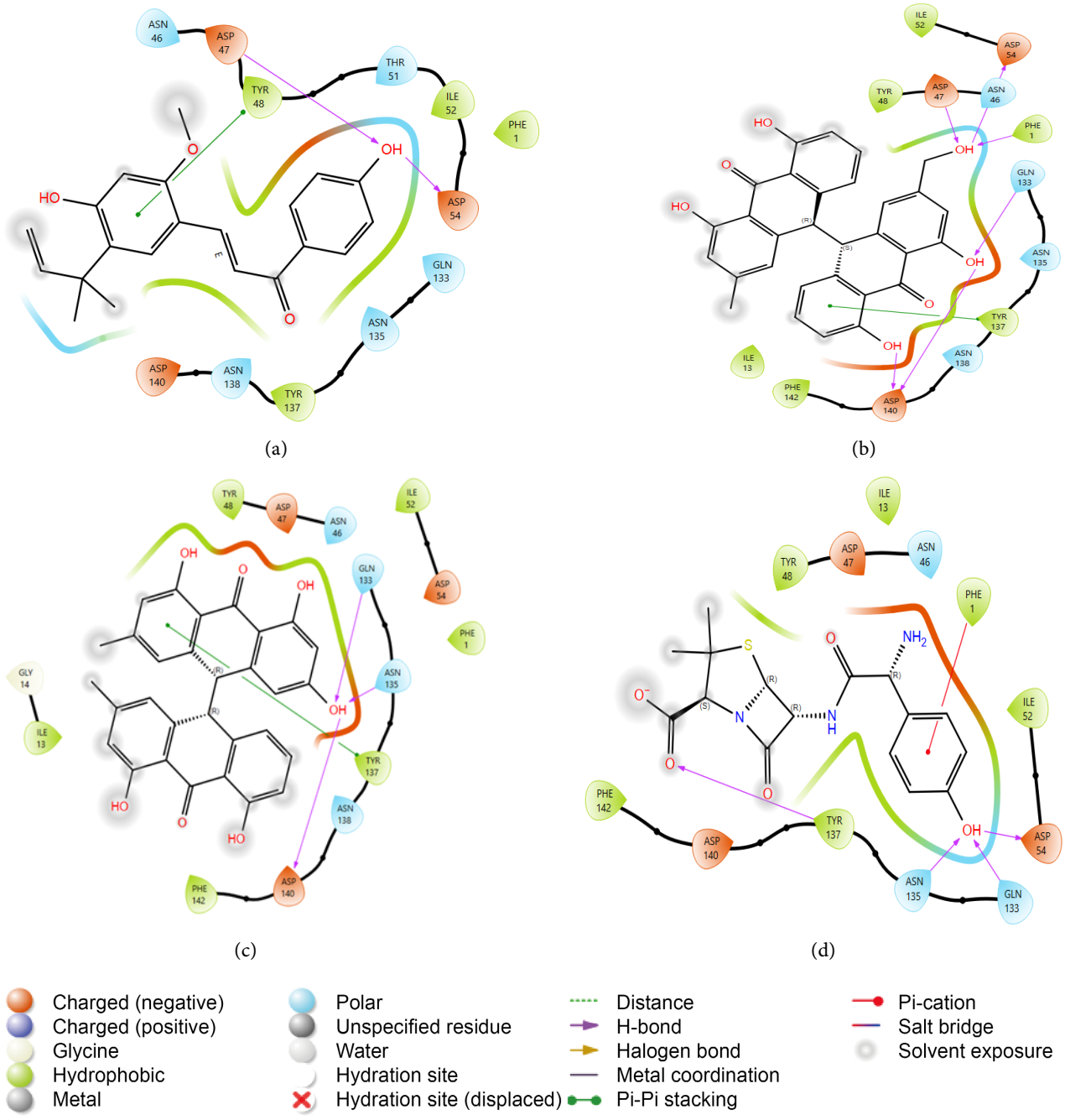

Figure 4. 2D interaction diagrams of different poses inside the binding pocket 8BVD for (a) Licochalcone A, (b) Palmidin B, (c) Palmidin C, (d) Amoxicillin.

a palmidin C oxygen atom. The ligand also exhibited hydrophobic interaction with Tyr137 polar residue. Inthis situation, the docking score of palmidin C seems to be more negative than that of palmidin B.

The fourth pose is the amoxicillin-target interaction, as shown in **Figure 4(d)**. This figure indicates that amoxicillin forms one OH group in the form of a hydrogen bond with Asp54, Asn135, Gln133 and an oxygen bond with Tyr137. In this case, the Asn135, and Gln133 polar residue acts as a hydrogen donor while

Asp54 act as hydrogen bond acceptor. Similarly, Tyr137 residues act as donor to amoxicillin oxygen atom. In this phenomenon, amoxicillin appears to be less negative than palmidin C compound.

In general, the complexity of protein-ligand interactions determines the strength of molecular docking (**Figure 3**) [43]. Licochalcone A forms hydrogen bonds with protein residues Asp47 and Asp54 which are more complex than those of palmidin B, which has three hydrogen bonds with Asp47, Asp54, Asn46, Phe1, G1n33, and Asp140, this ligand interacted with many residues compared to licochalcone A, Palmidin C and amoxicillin which formed a single hydrogen bond with Asp140, Asn135, Gln133, Asp54, Asn135 and Gln133, respectively. Nevertheless, the polar residue Tyr137 formed the covalent interaction with oxygen atoms from the amoxicillin drug a situation that made it more complex compared to palmidin C. Therefore, from the visual analysis, the best compound to form a ligand-target interaction was palmidin B, followed by licochalcone A, Palmidin C, and amoxicillin which were endorsed by the protein-ligand interaction docking scores (**Table 1**).

3.2. Physicochemical, Pharmacokinetics, Drug-Likeness and ADMET Prediction

For a molecule to be considered as a possible therapeutic candidate, it must possess the intended biological functions along with the best possible pharmacokinetics and safety profile [44]. One of the biggest challenges for oral medicine is its ability to cross the intestinal epithelial barrier, which affects the rate and degree of human absorption [45]. The selected compounds have an intestinal absorption rate of more than 89%, which is extremely high (**Table 2**). The chosen molecules also have non-hepatotoxic qualities, do not act as skin sensitizers, are non-permeable to the Blood Brain Barrier (BBB) and Central Nervous System (CNS), and are negative in AMES toxicity. It can also be reported that all ligands in this assessment permeate colon carcinoma cell 2 (CaCo-2) although Palmidin B, and Palmidin C seems to have a low penetration potential.

For the case of metabolism, the metabolic enzyme cytochrome P450 (CYP450) was tested and analyzed. The results show licochalcone A are potential inhibitors of CYP1A2, CYP2C9, CYP2C19, CYP3A4, and CYP1A2 while Palmidin B, and Palmidin C are potential inhibitor of CYP3A4 and CYP2C19 respectively. Toxic risk such as hepatotoxicity was also checked for all ligands, and the results from **Table 2** showed that the compounds cannot cause liver injury or impairment. Concerning the assessed results of inhibition of the hERG channel, it was noted that all ligands tested low toxic risk. The drug-likeness and EDMET properties jointly indicated that licochalcone A, Palmidin B, and Palmidin C might be potential candidates for preventing the target related to drug development against UTIs. According to recent data, licochalcone A is a natural flavonoid compound that has demonstrated its potential in the pharmacological aspects, it acts as an antioxidant, antitumor, and anti-inflammatory [46]. It prevents the proliferation

Table 2. ADMET prediction of the top-scored natural compounds.

Properties	Model name	Predicted Value				
		CID 5318998	CID 5320385	CID 5320386	CID 33613	Unit
Absorption	Water solubility	−4.528	−2.896	−2.901	−2.42	log mol/L
	P-gp substrate	Yes	No	No	No	-
	P-glycoprotein	Yes	Yes	Yes	Yes	-
	Gastrointestinal absorption	High	Low	Low	Low	-
	Caco2 permeability	0.699	−1.152	−1.138	0.245	cm/s
	Intestinal absorption (%)	91.243	98.848	89.268	37.356	-
	Skin Permeability	−2.837	−2.735	−2.735	−2.735	log Kp
Distribution	BBB permeability	−0.183	−0.982	−1.003	−1.06	-
	VDss (human)	0.313	−1.874	−2.119	−0.853	-
	Fraction unbound	0	0.295	0.262	0.753	-
	CNS permeability	−2.098	−3.242	−3.208	−3.345	-
Metabolism	Inhibitor CYP1A2	Yes	No	No	No	-
	CYP2C19	Yes	No	Yes	No	-
	CYP2C9	Yes	No	No	No	-
	CYP2D6	No	No	No	No	-
	CYP3A4	Yes	Yes	No	No	-
	CYP1A2	Yes	No	No	No	-
Excretion	Total Clearance	0.449	−0.253	−0.242	0.357	ml/min/kg
Toxicity	Renal OCT2 substrate	No	No	No	No	-
	Skin sensitization	No	No	No	No	-
	Hepatotoxicity	No	No	No	Yes	-
	AMES toxicity	No	No	No	No	-
	hERG I inhibitor	No	No	No	No	-
	hERG II inhibitor	No	Yes	Yes	No	-
	Minnow toxicity	0.72	2.616	2.884	4.969	log mM

of epithelial carcinoma and mesenchymal sarcoma cells. Palmidin B and palmidin C possess antibacterial, antifungal, antioxidant, anti-inflammatory, and anticancer activities [47].

3.3. Bioavailability Radar

The drug-likeness characteristics of an orally accessible, phytochemical medicine are graphically represented by bioavailability radar. The drug-likeness plots are displayed as a hexagon, with each vertex corresponding to a characteristic that describes a bioavailable medication [48]. The comprehensive and truthful tests

of licochalcone A, palmidin B, palmidin C and amoxicillin compounds were performed using swissADMEsoftware [49].

For a molecule to be classified as drug-like, its radar plot must lie within the colored zone. For each variable, the pink zone indicates the proper range, such as lipophilicity: XLOGP3 range between −0.7 to 5.0, molecular weight (MW) ranges between 150 and 500 g/mol, topological polar surface area (TPSA) ranges between 20 and 130 Å^2, solubility: logS less than 6, saturation (INSATU): fraction csp3 hybridization fraction greater than 0.25, and flexibility: less than 9 rotatable bonds (**Table 3**). Therefore, licochalcone A has oral bioavailability with slight unsaturation, while palmidin B and palmidin C seem to be more unsaturated in sp3 hybridization as a function of the carbon percentage with slight insoluble (**Figure 5**) [50].

3.4. Molecular Dynamics

Molecular dynamics (MD) was performed to examine the actual motion of atoms, which aids in understanding the detailed interaction of 8BVD with potential

Table 3. Physicochemical and drug-like properties analysis.

Descriptor/Properties	Value				
	CID 5318998	CID 5320385	CID 5320386	CID 33613	Units
Molecular weight	338.4	494.5	494.5	365.4	g/mol
Rotatable bonds	6	2	1	4	-
H. Acceptors	4	7	7	6	-
H. Donors	2	5	5	4	-
LogP	4.5112	4.36252	4.88424	0.0237	-
Num. arom. heavy atoms	12	24	24	6	-
Fraction Csp3	0.19	0.13	0.13	0.44	-
Num. of heavy atoms	25	37	24	25	
Topological polar surface area	66.76	135.29	135.29	158.26	Å^2
Molar refractivity	100.39	135.73	136.59	94.59	-

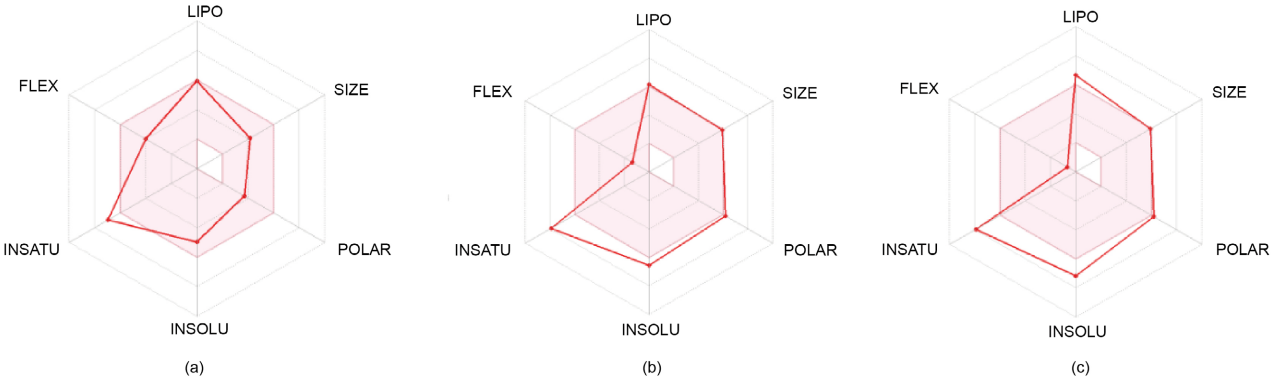

Figure 5. Bioavailability radar of the compounds (a) Licochalcone A, (b) Palmidin B, and (c) Palmidin C.

phytochemicals, especially when it binds to a protein target [51]. Several non-identified biological activities and intricate dynamic processes can be discovered by observing the internal dynamics of proteins [52].

3.5. Hydrogen Bonding (H-Bonds) Analysis

The essential component of understanding molecular interactions, especially in biomolecular system, is hydrogen bond investigation. It aids in the comprehension of the nature and strength of hydrogen bonds inside the molecular structures [53]. Hydrogen bond analysis can also be used to examine the strength of the protein-ligand complex to assess the molecular recognition, directionality, and specificity of contacts [54].

The analysis from **Figure 6** showed that licochalcone A formed a maximum of 5-H bonds during the molecular dynamics computation. It formed 1 to 4 hydrogen bonds from 0 to 20 ns. The hydrogen bonds formed between 1 and 3 were the most stable compared with the ones formed between 3 and 5 which had higher fluctuations (**Figure 6(a)**). The higher electrostatic forces might contribute to the stability of the hydrogen bonds.

Palmidin B formed a maximum of 2 hydrogen bonds during MD simulation. From 0 to 20 ns one (1) hydrogen bond was formed. This was the most stable hydrogen bond of this compound compared with the hydrogen bond formed between 1 and 2 which had higher fluctuations. The fluctuations might be contributed by the high electronegative atoms of this compound (**Figure 6(b)**).

Palmidin C formed two (2) hydrogen bonds during this computational analysis. In between 0 to 20 ns one (1) hydrogen bond was formed. This hydrogen bond was the most stable compared with the hydrogen bond formed between 1 and 2 which had greater fluctuations (**Figure 6(c)**).

Amoxicillin formed 7-H bonds during the molecular dynamics computation. 6-H bond was formed from 0 to 5 ns with slight fluctuations while the 4-H bond was formed from 5 to 20 ns with some fluctuations. The hydrogen bond formed from 2 to 3 was the most stable for 20 ns. Principally, all four ligands had good H-bonding with the active pocket 8BVD; however, licochalcone A had the most stable H-bonding compared to other ligands (**Figure 6(d)**).

3.6. Root Mean Square Deviation (RMSD)

The root mean square deviation of each trajectory record for 20000 ps (20 ns) in the MD simulation was calculated with respect to the protein ligand's initial position to determine the stability of the docked complex [55].

From the trajectory analysis, licochalcone A appeared to bind more stable with the target molecule at 0.7 nm, although the ligand had slight destabilization at 6.5 ns to 12.5 ns before maintained stability at 0.7 nm from 13 ns up to 20 ns. The mean RMSD for licochalcone A was attained at 0.55 nm. Palmidin B exhibited stability at 1 nm from 0 to 2.5 ns, then fluctuated from 1 up to 5 nm from 2.6 ns to 7.5 ns, then regained stability at 7.5 to 20 ns. The mean value was recorded at 0.83 nm. Palmidin C had better stability compared with Palmidin B, the

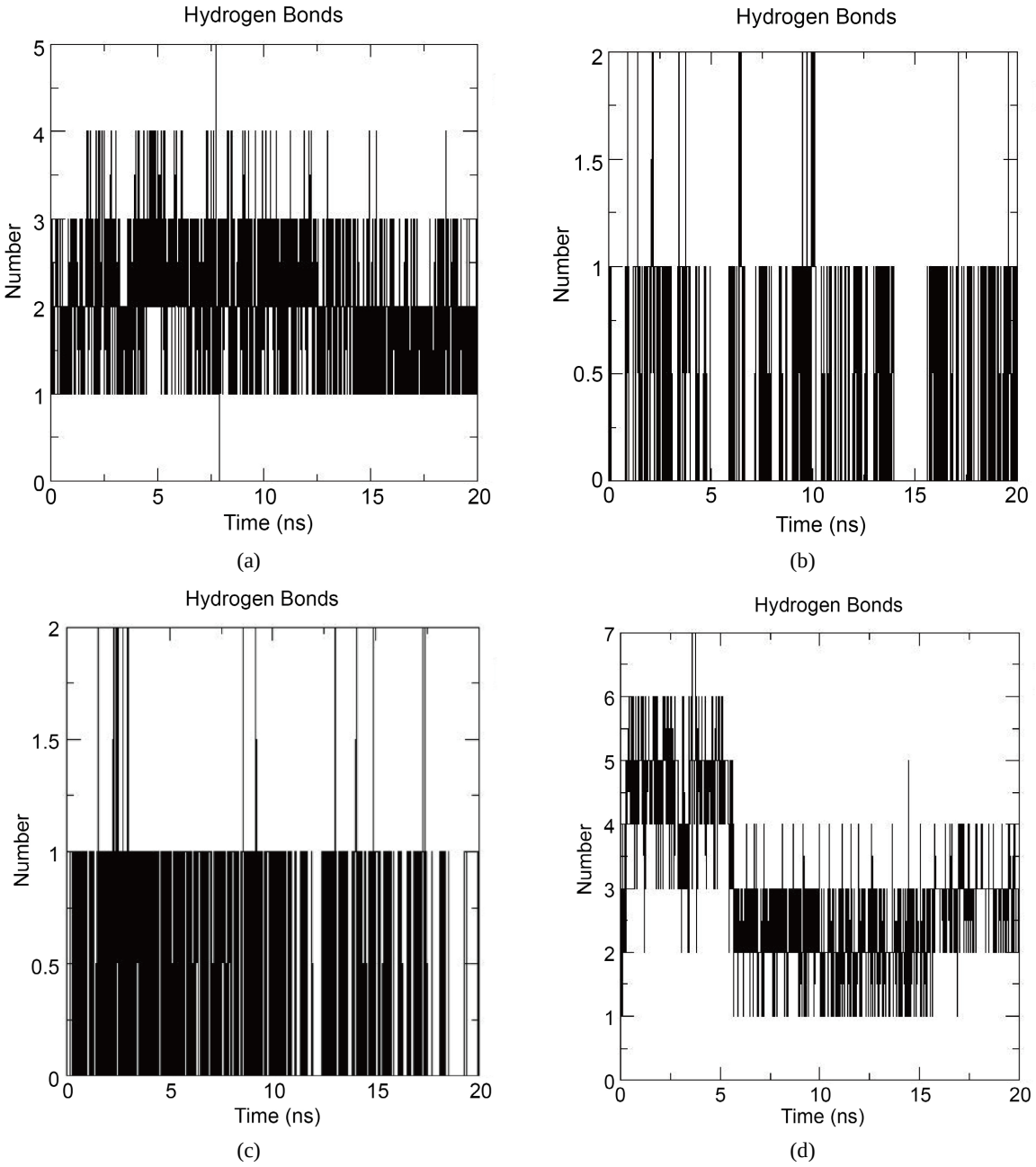

Figure 6. Hydrogen bonds formed by (a) licochalcone A, (b) palmidin B, (c) palmidin C and (d) amoxicillin.

ligand binds with the 8BVD target at 1 nm and maintained stability up to 7.5 ns, and then after 7.5 ns the ligand had slight fluctuation from 1 to 0.3 nm and maintained it from 7.5 ns to 17.5 ns. The mean value was observed at 0.53 nm. RMSD for Amoxicillin ligands was stable at 0.75 nm from 0 to 20 ns (**Figure 7**). Looking at the three ligands, Palmidin C was the most stable compared with other ligands.

3.7. Root Mean Square Fluctuation (RMSF)

RMSF determines the movement of an individual atom or group of atoms from

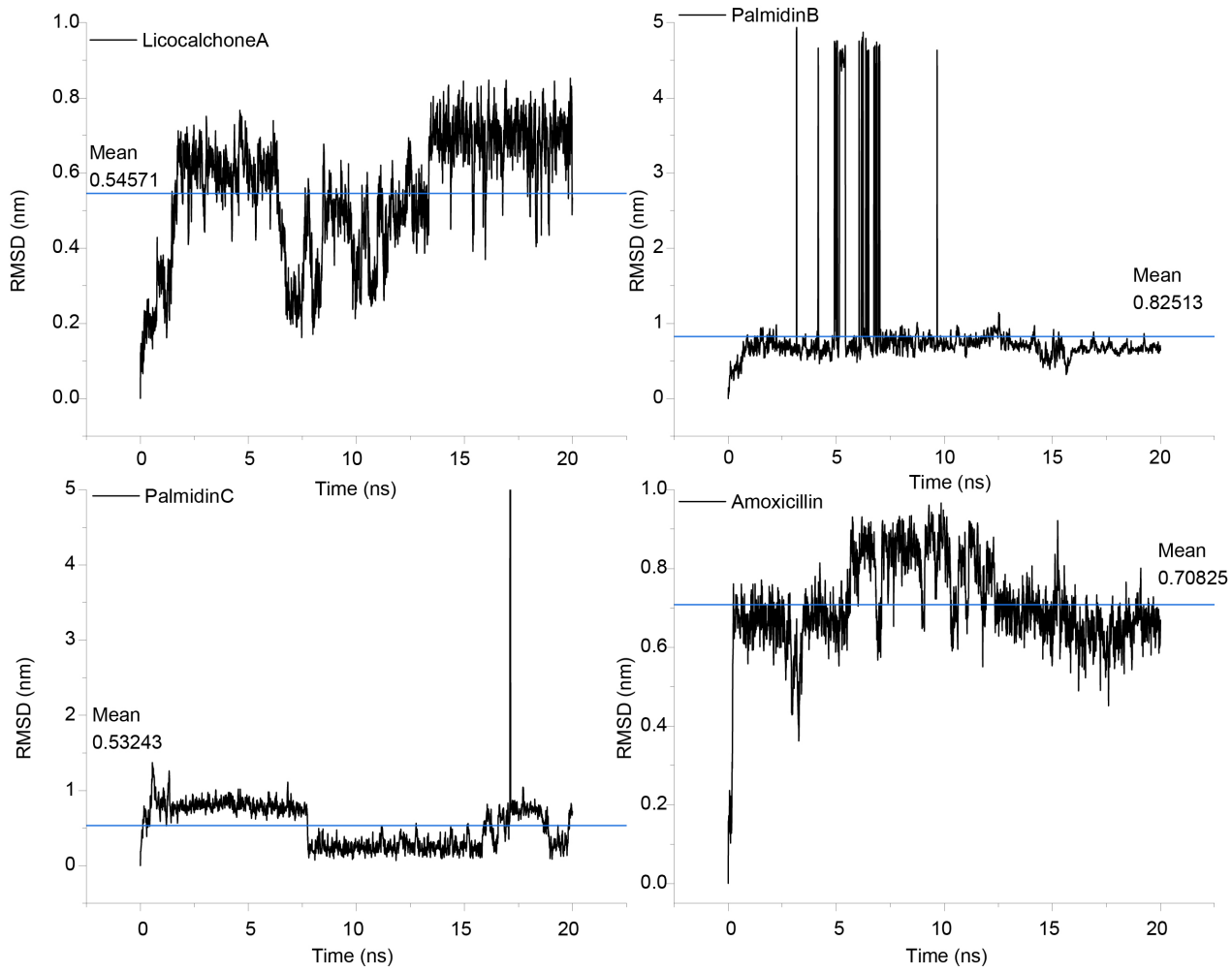

Figure 7. RMSD for Licochalcone A, Palmidin B, Palmidin C and amoxicillin ligands.

the reference structure across the total number of atoms [55] [56]. It is commonly used to determine if a structure is departing from the initial coordinates or stable within the simulation time scale [56]. It is worthwhile to analyze the time-dependent motions of the structures. To forecast the stable structure, the RMSF was calculated using the GROMACS standard function, and the fluctuations of various atoms were examined for 20 ns.

Analysis of the RMSF shows that the HC5 atom of licochalcone A fluctuated more than the other atoms. The RMSF value of the HC5 atom was 0.25 nm, followed by H22 and HC15, both with RMSF value of 0.23 nm while the H18, atom fluctuated at an RMSF value of 0.22 nm. Those atoms that fluctuated more were at the terminals of the aromatic rings.

The H22 atom of Palmidin B was observed to have the highest fluctuation at an RMSF value of 0.19 nm, followed by HC13 and HC12 with RMSF values of 0.13 and 0.12 nm, respectively while C16, C15, and HC14 exhibited RMSF values of 0.12, nm. The other atoms are stable at an average RMSF value of 0.03 nm.

For the case of Palmidin C, the HC15 atom had a higher fluctuation with an

RMSF value of 0.12 nm, followed by HC16, and HC14 atoms with RMSF values of 0.119 nm each. Equally, atoms such as H22, H21, and H19 also fluctuated with RMSF values of 0.10, 0.079 and 0.06 nm, respectively. Other atoms of this ligand were stable at the average RMSF of 0.03 nm.

The HC9 atom of the amoxicillin unveiled higher fluctuation at the RMSF value of 0.14 nm, atoms like HC8, and HC10 had the RMSF value of 0.13 nm each while other atoms such as HC12 and HC19 have an RMSF value of 0.12 nm each. The average RMSF value for the other atoms was recorded at 0.06 nm (Figure 8).

3.8. Radius of Gyration (Rg)

The radius of gyration (Rg) determines the strength of the protein. In the protein-ligand complex, the radius of gyration of a ligand shows the ligand center of gyration to the center of gyration of the protein; therefore, a higher value of the radius of gyration indicates less stability of the structure [57]. The results show

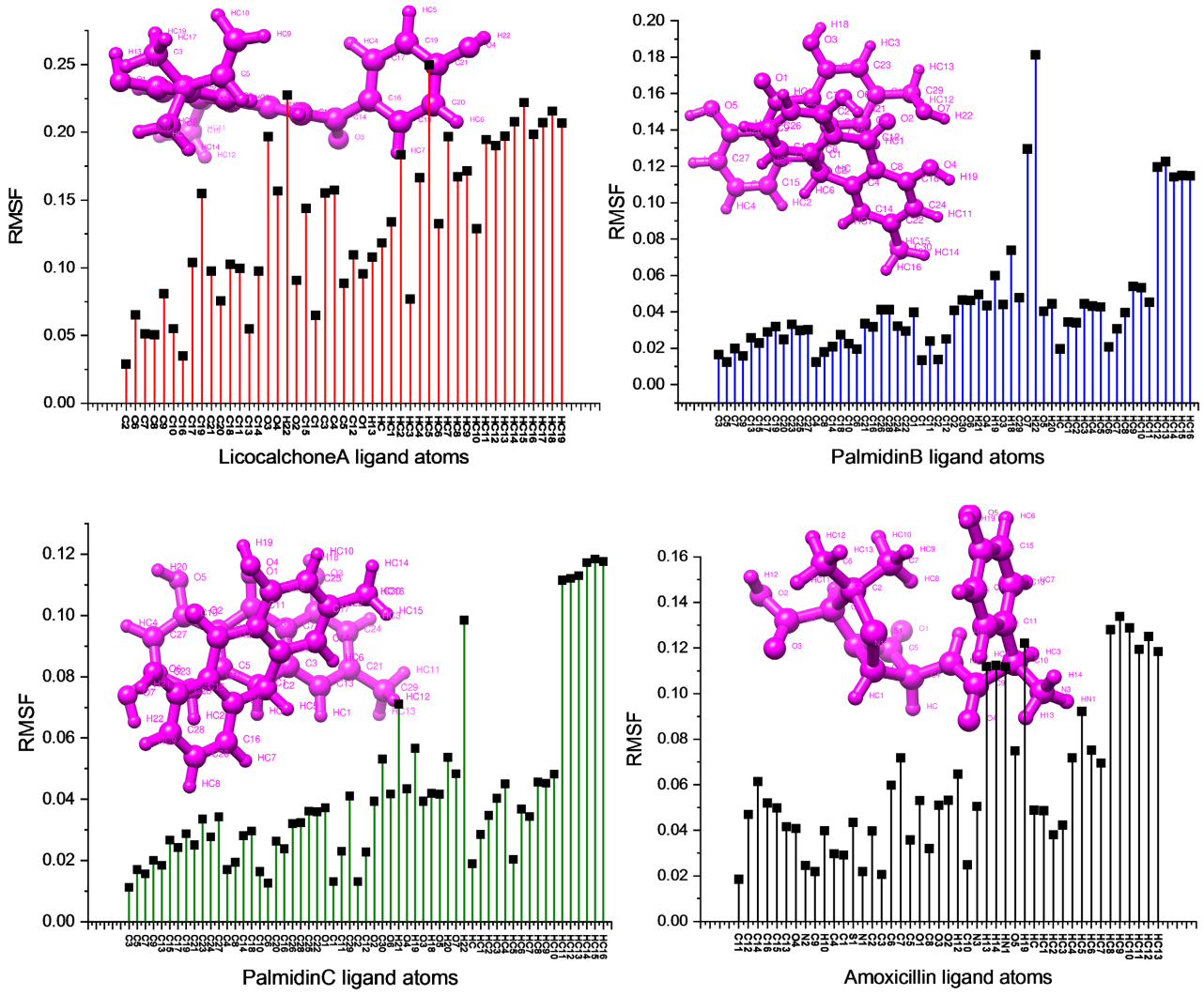

Figure 8. RMSF for licochalcone A, palmidin B, palmidin C and amoxicillin ligands.

that licochalcone A gyrated at 0.45 nm which is higher compared to the other three ligands. Other ligands like palmidin B, palmidin C, and amoxicillin seem to be stable at the average Rg value of 0.38 nm (Figure 9).

3.9. Potential Energy

The relative potential energy can be used to compare conformations and configurations of the molecular system. Potential energies of the system of both proteins and ligands were plotted as a function of MD simulation time, and the plots are shown in Figure 10. The results from the plot illustrate that palmidin B is more stable than the other three ligands, with a total energy of −318000 kJ/mol. Licochalcone A, palmidin C and amoxicillin ligands were also stable, with slightly higher energies ranging from −314000 to −308000 KJ/mol (Figure 10).

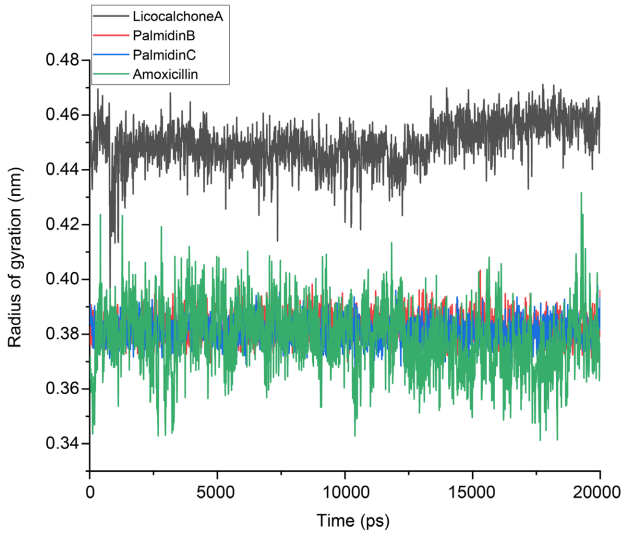

Figure 9. Radius of gyration for licochalcone A, palmidin B, palmidin C and amoxicillin ligands.

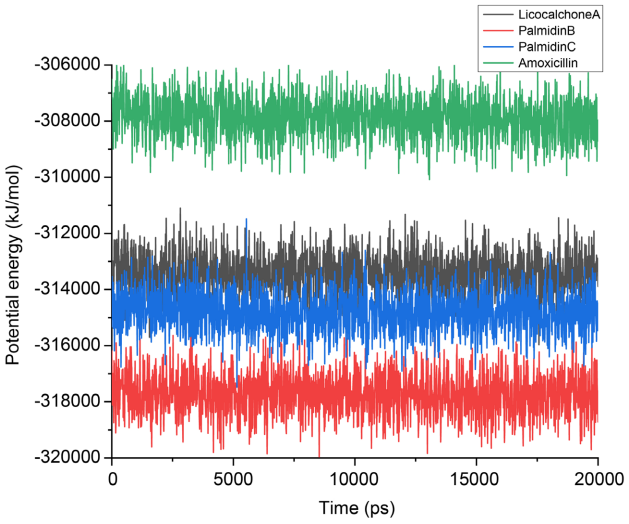

Figure 10. Potential energies of the system during the MD simulation.

The lower energy of the trajectory profile indicates that the system was considerably stable throughout the simulation [58].

4. Conclusion

Natural compounds are the most important source of medicines for the treatment of many diseases [59]. Molecular docking and molecular dynamics were successfully performed on the ligand-target complex. Based on the molecular docking scores, ADMET studies, and drug-like properties, all ligands were excellent candidates as 8BVD inhibitors. The order of docking scores ranged from high to low as follows; licochalcone A, palmidin C, palmidin B and amoxicillin. However, looking at the ligand-target interaction and the MD simulation analysis it can be concluded that palmidin C had a better chance of being considered as a suitable drug candidate compared with the other ligands. Nevertheless, more studies are still needed to confirm the precise mechanisms and outcomes of UTI treatment through clinical and experimental validation.

Funding Support

The authors gratefully acknowledge the Tanzanian Atomic Energy Commission (TAEC) for providing the funding necessary to complete this project.

Conflicts of Interest

The authors declare no conflicts of interest regarding the publication of this paper.

References

[1] Indu, S., Surajit, C. and Sagolsem, Y. (2021) *In Silico* Screening of Some Phytochemicals for Treating Urinary Tract Infection (UTI) Targeting fimH Gene. *African Journal of Bioscience*, **3**, 157-164. https://ssrn.com/abstract=3772355 https://doi.org/10.33472/AFJBS.3.1.2021.157-164

[2] Arsene, M.M.J., Viktorovna, P.I., Sergei, G.V., Hajjar, F., Vyacheslavovna, Y.N., Vladimirovna, Z.A., Aleksandrovna, V.E., Nikolayevich, S.A. and Sachivkina, N. (2022) Phytochemical Analysis, Antibacterial and Antibiofilm Activities of *Aloe vera* Aqueous Extract against Selected Resistant Gram-Negative Bacteria Involved in Urinary Tract Infections. *Fermentation*, **8**, Article 626. https://doi.org/10.3390/fermentation8110626

[3] Jagdish, R. and Nehra, K. (2022) *Bryophyllumpinnatum* Mediated Synthesis of Zinc Oxide Nanoparticles: Characterization and Application as Biocontrol Agents for Multi-Drug-Resistant Uropathogens. *Heliyon*, **8**, E11080. https://doi.org/10.1016/j.heliyon.2022.e11080

[4] Khoshkbejari, M., Jafari, A. and Safari, M. (2015) Ag/ZnO Nanoparticles as Novel Antibacterialagent against of *Escherichia Coli* Infection, *in Vitro* & *in Vivo*. *Oriental Journal of Chemistry*, **31**, 1437-1445. https://doi.org/10.13005/ojc/310322

[5] Flores-Mireles, A.L., Walker, J.N., Caparon, M. and Hultgren, S.J. (2015) Urinary Tract Infections: Epidemiology, Mechanisms of Infection and Treatment Options. *Nature Reviews Microbiology*, **13**, 269-284. https://doi.org/10.1038/nrmicro3432

[6] Zagaglia, C., Ammendolia, M.G., Maurizi, L., Nicoletti, M. and Longhi, C. (2022) Urinary Tract Infections Caused by Uropathogenic *Escherichia coli* Strains—New Strategies for an Old Pathogen. *Microorganisms*, **10**, Article 1425. https://doi.org/10.3390/microorganisms10071425

[7] Storme, O., Tirán Saucedo, J., Garcia-Mora, A., Dehesa-Dávila, M. and Naber, K.G. (2019) Risk Factors and Predisposing Conditions for Urinary Tract Infection. *Therapeutic Advances in Urology*, **11**, 19-28. https://doi.org/10.1177/1756287218814382

[8] Jaiswal, S.K., Sharma, N.K., Bharti, S.K., Krishnan, S., Kumar, A., Prakash, O., Kumar, P., Kumar, A. and Gupta, A.K. (2018) Phytochemicals as Uropathognic *Escherichia Coli* FimH Antagonist: *In Vitro* and *in Silico* Approach. *Current Molecular Medicine*, **18**, 640-653. https://doi.org/10.2174/1566524019666190104104507

[9] Derakhshandeh, A., Firouzi, R., Motamedifar, M., Motamedi Boroojeni, A., Bahadori, M., Arabshahi, S., Novinrooz, A. and Heidari, S. (2015) Distribution of Virulence Genes and Multiple Drug-Resistant Patterns amongst Different Phylogenetic Groups of Uropathogenic *Escherichia coli* Isolated from Patients with Urinary Tract Infection. *Letters in Applied Microbiology*, **60**, 148-154. https://doi.org/10.1111/lam.12349

[10] Hojati, Z., Zamanzad, B., Hashemzadeh, M., Molaie, R. and Gholipour, A. (2015) Detection of FimH Gene in Uropathogenic *Escherichia coli* Strains Isolated from Patients with Urinary Tract Infection. *Journal of Microbiology*, **8**, e17520. https://doi.org/10.5812/jjm.17520

[11] Shah, C., Baral, R., Bartaula, B. and Shrestha, L.B. (2019) Virulence Factors of Uropathogenic *Escherichia coli* (UPEC) and Correlation with Antimicrobial Resistance. *BMC Microbiology*, **19**, Article No. 204. https://doi.org/10.1186/s12866-019-1587-3

[12] Gupta, K., Hooton, T.M., Naber, K.G., Wullt, B., Colgan, R., Miller, L.G., Moran, G.J., Nicolle, L.E., Raz, R., Schaeffer, A.J. and Soper, D.E. (2011) International Clinical Practice Guidelines for the Treatment of Acute Uncomplicated Cystitis and Pyelonephritis in Women: A 2010 Update by the Infectious Diseases Society of America and the European Society for Microbiology and Infectious Diseases. *Clinical Infectious Diseases*, **52**, e103-e120. https://doi.org/10.1093/cid/ciq257

[13] Stanton, I.C., Bethel, A., Leonard, A.F.C., Gaze, W.H. and Garside, R. (2020) What Is the Research Evidence for Antibiotic Resistance Exposure and Transmission to Humans from the Environment? A Systematic Map Protocol. *Environmental Evidence*, **9**, Article No. 12. https://doi.org/10.1186/s13750-020-00197-6

[14] Warren, J.W., Abrutyn, E., Hebel, J.R., Johnson, J.R., Schaeffer, A.J. and Stamm, W.E. (1999) Guidelines for Antimicrobial Treatment of Uncomplicated Acute Bacterial Cystitis and Acute Pyelonephritis in Women. *Clinical Infectious Diseases*, **29**, 745-759. https://doi.org/10.1086/520427

[15] Bathaie, S.Z., Faridi, N., Nasimian, A., Heidarzadeh, H. and Tamanoi, F. (2015) How Phytochemicals Prevent Chemical Carcinogens and/or Suppress Tumor Growth? *The Enzymes*, 37, 1-42. https://doi.org/10.1016/bs.enz.2015.06.003

[16] Fatriansyah, J.F., Rizqillah, R.K., Yandi, M.Y. and Muhamad Sahlan, F. (2022) Molecular Docking and Dynamics Studies on Propolis Sulabiroin-A as a Potential Inhibitor of SARS-CoV-2. *Journal of King Saud University—Science*, **34**, Article ID: 101707. https://doi.org/10.1016/j.jksus.2021.101707

[17] Yu, W. and MacKerell Jr., A.D. (2017) Computer-Aided Drug Design Methods. In: Sass, P., Ed., *Antibiotics*, Humana Press, New York, 85-106. https://doi.org/10.1007/978-1-4939-6634-9_5

[18] Preman, G., Mulani, M., Bare, A., Relan, K., Sayyed, L., Jha, V. and Pandey, K. (2022) Virtual Screening of Phytochemicals for Anti-Tubercular Potential Using Molecular Docking Approach. *Journal of Tuberculosis*, **5**, 1030.

[19] Sliwoski, G., Kothiwale, S., Meiler, J. and Lowe Jr., E.W. (2013) Computational Methods in Drug Discovery. *Pharmacological Reviews*, **66**, 334-395. https://doi.org/10.1124/pr.112.007336

[20] Bittner Fialová, S., Rendeková, K., Mučaji, P., Nagy, M. and Slobodníková, L. (2021) Antibacterial Activity of Medicinal Plants and Their Constituents in the Context of Skin and Wound Infections, Considering European Legislation and Folk Medicine—A Review. *International Journal of Molecular Sciences*, **22**, Article 10746. https://doi.org/10.3390/ijms221910746

[21] Goudarzi, M., Ghafari, S., Navidinia, M. and Azimi, H. (2018) *Aloe vera* Gel: Effective Therapeutic Agent against Extended-Spectrum *β*-Lactamase Producing *Escherichia coli* Isolated from Patients with Urinary Tract Infection in Tehran-Iran. *Journal of Pure and Applied Microbiology*, **11**, 1401-1408. https://doi.org/10.22207/JPAM.11.3.22

[22] Newman, D.J. and Cragg, G.M. (2020) Natural Products as Sources of New Drugs over the Nearly Four Decades from 01/1981 to 09/2019. *Journal of Natural Products*, **83**, 770-803. https://doi.org/10.1021/acs.jnatprod.9b01285

[23] Mousavifar, L., Sarshar, M., Bridot, C., Scribano, D., Ambrosi, C., Palamara, A.T., Vergoten, G., Roubinet, B., Landemarre, L., Bouckaert, J. and René, R. (2023) Insightful Improvement in the Design of Potent Uropathogenic *E. coli* FimH Antagonists. *Pharmaceutics*, **15**, Article 527. https://doi.org/10.3390/pharmaceutics15020527

[24] Liebschner, D., Afonine, P.V., Baker, M.L., Bunkóczi, G., Chen, V.B., Croll, T.I., Hintze, B., Hung, L.W., Jain, S., McCoy, A.J., *et al.* (2019) Macromolecular Structure Determination Using X-Rays, Neutrons and Electrons: Recent Developments in Phenix. *Acta Crystallographica*, **D75**, 861-877. https://doi.org/10.1107/S2059798319011471

[25] Kleywegt, G.J. and Jones, T.A. (1997) Model Building and Refinement Practice. *Methods in Enzymology*, **277**, 208-230. https://doi.org/10.1016/S0076-6879(97)77013-7

[26] Abe, C.M., Salvador, A., Falsetti, I.N., Blanco, E. and Blanco, M. (2008) Uropathogenic *Escherichia coli* (UPEC) Strains May Carry Virulence Properties of Diarrhoeagenic *E. coli*. *FEMS Immunology & Medical Microbiology*, **52**, 397-406. https://doi.org/10.1111/j.1574-695X.2008.00388.x

[27] Pettersen, E.F., Goddard, T.D., Huang, C.C., Couch, G.S., Greenblatt, D.M., Meng, E.C. and Ferrin, T.E. (2004) UCSF Chimera—A Visualization System for Exploratory Research and Analysis. *Journal of Computational Chemistry*, **25**, 1605-1612. https://doi.org/10.1002/jcc.20084

[28] Huang, C.C., Couch, G.S., Pettersen, E.F. and Chimera, F.T.E. (1996) An Extensible Molecular Modeling Application Constructed Using Standard Components. *Pacific Symposium on Biocomputing*, **1**, Article 724.

[29] Zafar, F., Gupta, A., Thangavel, K., Khatana, K., Sani, A.A., Ghosal, A., Tandon, P. and Nishat, N. (2020) Physicochemical and Pharmacokinetic Analysis of Anacardic Acid Derivatives. *ACS Omega*, **5**, 6021-6030. https://doi.org/10.1021/acsomega.9b04398

[30] Camp, D., Garavelas, A. and Campitelli, M. (2015) Analysis of Physicochemical Properties for Drugs of Natural Origin. *Journal of Natural Products*, **78**, 1370-1382.

https://doi.org/10.1021/acs.jnatprod.5b00255

[31] Honório, K.M., Moda, T.L. and Andricopulo, A.D. (2013) Pharmacokinetic Properties and *in Silico* ADME Modeling in Drug Discovery. *Medicinal Chemistry*, **9**, 163-176. https://doi.org/10.2174/1573406411309020002

[32] Jia, C.Y., Li, J.Y., Hao, G.F. and Yang, G.F. (2020) A Drug-Likeness Toolbox Facilitates ADMET Study in Drug Discovery. *Drug Discovery Today*, **25**, 248-258. https://doi.org/10.1016/j.drudis.2019.10.014

[33] Pires, D.E.V., Blundell, T.L. and Ascher, D.B. (2015) Predicting Small-Molecule Pharmacokinetic and Toxicity Properties Using Graph-Based Signatures. *Journal of Medicinal Chemistry*, **58**, 4066-4072. https://doi.org/10.1021/acs.jmedchem.5b00104

[34] Oomariyah, N. and van Dijk, G. (2022) The Bioavailability Prediction and Screening Phytochemicals of Sansevieria Trifasciata Leaves Extract. *MATEC Web of Conferences*, **372**, Article ID: 02003. https://doi.org/10.1051/matecconf/202237202003

[35] Udugade, S.B., Doijad, R.C. and Udugade, B.V. (2019) *In Silico* Evaluation of Pharmacokinetics, Drug-Likeness and Medicinal Chemistry Friendliness of Momordicin1: An Active Chemical Constituent of Momordica Charantia. *Journal of Advanced Scientific Research*, **10**, 222-229.

[36] Leach, A.R. (2007) Ligand-Based Approaches: Core Molecular Modeling. *Comprehensive Medicinal Chemistry II*, **4**, 87-118. https://doi.org/10.1016/B0-08-045044-X/00246-7

[37] Hansson, T., Oostenbrink, C. and van Gunsteren, W. (2002) Molecular Dynamics Simulations. *Current Opinion in Structural Biology*, **12**, 190-196. https://doi.org/10.1016/S0959-440X(02)00308-1

[38] Hess, B., Kutzner, C., Van Der Spoel, D. and Lindahl, E. (2008) GROMACS 4: Algorithms for Highly Efficient, Load-Balanced, and Scalable Molecular Simulation. *Journal of Chemical Theory and Computation*, **4**, 435-447. https://doi.org/10.1021/ct700301q

[39] Van Der Spoel, D., Lindahl, E., Hess, B., Groenhof, G., Mark, A.E. and Berendsen, H.J. (2005) GROMACS: Fast, Flexible, and Free. *Journal of Computational Chemistry*, **26**, 1701-1718. https://doi.org/10.1002/jcc.20291

[40] Salaria, D., Rolta, R., Mehta, J., Awofisayo, O., Fadare, O.A., Kaur, B., Kumar, B., Araujo da Costa, R., Chandel, S.R., Kaushik, N., Choi, E.H. and Kaushik, N.K. (2022) Phytoconstituents of Traditional Himalayan Herbs as Potential Inhibitors of Human Papillomavirus (HPV-18) for Cervical Cancer Treatment: An *in Silico* Approach. *PLOS ONE*, **17**, e0265420. https://doi.org/10.1371/journal.pone.0265420

[41] Galande, A.K. and Rohane, S.H. (2021) Insilico Molecular Docking Analysis in Maestro Software. *Asian Journal of Research in Chemistry*, **14**, 97-100. https://doi.org/10.5958/0974-4150.2021.00017.1

[42] Olloquequi, J., Ettcheto, M., Cano, A., Fortuna, A., Bicker, J., Sánchez-Lopez, E., Paz, C., Ureña, J., Verdaguer, E., Auladell, C., *et al*. (2023) Licochalcone A: A Potential Multitarget Drug for Alzheimer's Disease Treatment. *International Journal of Molecular Sciences*, **24**, Article 14177. https://doi.org/10.3390/ijms241814177

[43] Li, M.T., Xie, L., Jiang, H.M., Huang, Q., Tong, R.S., Li, X., Xie, X. and Liu, H.M. (2022) Role of Licochalcone a in Potential Pharmacological Therapy: A Review. *Frontiers in Pharmacology*, **13**, Article 878776. https://doi.org/10.3389/fphar.2022.878776

[44] Madeddu, F., Di Martino, J., Pieroni, M., Del Buono, D., Bottoni, P., Botta, L., Ca-

strignanò, T. and Saladino, R. (2022) Molecular Docking and Dynamics Simulation Revealed the Potential Inhibitory Activity of New Drugs against Human Topoisomerase I Receptor. *International Journal of Molecular Sciences*, **23**, Article 14652. https://doi.org/10.3390/ijms232314652

[45] Hu, Q., Feng, M., Lai, L. and Pei, J. (2018) Prediction of Drug-Likeness Using Deep Autoencoder Neural Networks. *Frontiers in Genetics*, **9**, Article 422486. https://doi.org/10.3389/fgene.2018.00585

[46] Lin, J.H., Yang, K.T., Ting, P.C., Lee, W.S., Lin, D.J. and Chang, J.C. (2023) Licochalcone a Improves Cardiac Functions after Ischemia-Reperfusion via Reduction of Ferroptosis in Rats. *European Journal of Pharmacology*, **957**, Article ID: 176031. https://doi.org/10.1016/j.ejphar.2023.176031

[47] Daniyal, M., Mahmood Tahir, I., Akram, M., Zahid, R., Zainab, R., Riaz, Z., Laila, U., Riaz, T., Wang, W. and Bin, L. (2019) Pharmacological Effects of Rheum Emodi: A Multiple Purpose Plant in Health and Disease. *Journal of Medical and Biological Sciences*, **2**, 68-73.

[48] Rao, P., Shukla, A., Parmar, P., Rawal, R.M., Patel, B., Saraf, M. and Goswami, D. (2020) Reckoning a Fungal Metabolite, Pyranonigrin A as a Potential Main Protease (Mpro) Inhibitor of Novel SARS-CoV-2 Virus Identified Using Docking and Molecular Dynamics Simulation. *Biophysical Chemistry*, **264**, Article ID: 106425. https://doi.org/10.1016/j.bpc.2020.106425

[49] Ndombera, F.T., Maiyoh, G.K.K. and Tuei, V.C. (2019) Pharmacokinetic, Physicochemical and Medicinal Properties of N-Glycoside Anti-Cancer Agent More Potent than 2-Deoxy-D-Glucose in Lung Cancer Cells. *Journal of Pharmacy and Pharmacology*, **7**, 165-176. https://doi.org/10.17265/2328-2150/2019.04.003

[50] Daina, A., Michielin, O. and Zoete, V. (2017) SwissADME: A Free Web Tool to Evaluate Pharmacokinetics, Drug-Likeness and Medicinal Chemistry Friendliness of Small Molecules. *Scientific Reports*, **7**, Article No. 42717. https://doi.org/10.1038/srep42717

[51] Hansson, T., Oostenbrink, C. and van Gunsteren, W.F. (2002) Molecular Dynamics Simulations. *Current Opinion in Structural Biology*, **12**, 190-196. https://doi.org/10.1016/S0959-440X(02)00308-1

[52] Anwer, K., Sonani, R., Madamwar, D., Singh, P., Khan, F., Bisetty, K., Ahmad, F. and Hassan, M.I. (2015) Role of N-Terminal Residues on Folding and Stability of C-Phycoerythrin: Simulation and Urea-Induced Denaturation Studies. *Journal of Biomolecular Structure and Dynamics*, **33**, 121-133. https://doi.org/10.1080/07391102.2013.855144

[53] GROMACS Tutorial: Coarse-Grained Simulation of a Protein Membrane System. https://www.compchems.com/hydrogen-bond-analysis-with-vmd/#step-6-analyzing-the-results

[54] Mohammad, T., Siddiqui, S., Shamsi, A., Alajmi, M.F., Hussain, A., Islam, A., Ahmad, F. and Hassan, M.I. (2020) Virtual Screening Approach to Identify High-Affinity Inhibitors of Serum and Glucocorticoid-Regulated Kinase 1 among Bioactive Natural Products: Combined Molecular Docking and Simulation Studies. *Molecules*, **25**, Article 823. https://doi.org/10.3390/molecules25040823

[55] Anusuya, S., Velmurugan, D. and Gromiha, M.M. (2015) Identification of Dengue Viral RNA-Dependent RNA Polymerase Inhibitor Using Computational Fragment Based Approaches and Molecular Dynamics Study. *Journal of Biomolecular Structure and Dynamics*, **34**, 1512-1532. https://doi.org/10.1080/07391102.2015.1081620

[56] Martínez, L. (2015) Automatic Identification of Mobile and Rigid Substructures in

Molecular Dynamics Simulations and Fractional Structural Fluctuation Analysis. *PLOS ONE*, **10**, e0119264. https://doi.org/10.1371/journal.pone.0119264

[57] Lobanov, M.Y., Bogatyreva, N.S. and Galzitskaya, O.V. (2008) Radius of Gyration as an Indicator of Protein Structure Compactness. *Molecular Biology*, **42**, 623-628. https://doi.org/10.1134/S0026893308040195

[58] Lakshmi, S.A., Shafreen, R.M.B., Priya, A. and Shunmugiah, K.P. (2021) Ethnomedicines of Indian Origin for Combating COVID-19 Infection by Hampering the Viral Replication: Using Structure-Based Drug Discovery Approach. *Journal of Biomolecular Structure and Dynamics*, **39**, 4594-4609. https://doi.org/10.1080/07391102.2020.1778537

[59] Veeresham, C. (2012) Natural Products Derived from Plants as a Source of Drugs. *Journal of Advanced Pharmaceutical Technology & Research*, **3**, 200-201. https://doi.org/10.4103/2231-4040.104709